The Cryosphere
Open Access
Discussions

Influence of meltwater input on the skill of decadal forecast of sea ice in the Southern Ocean

V. Zunz[1,*] and H. Goosse[1]

[1]Université catholique de Louvain, Earth and Life Institute, Georges Lemaître Centre for Earth and Climate Research, Louvain-la-Neuve, Belgium

[*]*Invited contribution by V. Zunz, recipient of the EGU Young Scientists Outstanding Poster Paper Award 2013.*

Correspondence to: V. Zunz (violette.zunz@uclouvain.be)

TCD

8, 3563–3602, 2014

Decadal forecast skill of Southern Ocean sea ice

V. Zunz and H. Goosse

Title Page

Abstract	Introduction
Conclusions	References
Tables	Figures

|◄ | ►|

◄ | ►

Back | Close

Full Screen / Esc

Printer-friendly Version

Interactive Discussion

Abstract

Recent studies have investigated the potential link between the freshwater input derived from the melting of the Antarctic ice sheet and the observed recent increase in sea ice extent in the Southern Ocean. In this study, we assess the impact of an additional freshwater flux on the trend in sea ice extent and concentration in a simulation with data assimilation, spanning the period 1850–2009, as well as in retrospective forecasts (hindcasts) initialised in 1980. In a simulation with data assimilation, including an additional freshwater flux that follows an autoregressive process improves the reconstruction of the trend in ice extent and concentration between 1980 and 2009. This is partly due to a better representation of the freshwater cycle in the Southern Ocean, but the additional flux could also compensate for some model deficiencies. In addition, it modifies the simulated mean state of the sea ice. A hindcast initialised from this shifted state has to be forced by an additional freshwater flux with an amplitude similar to the one included in the simulation with data assimilation in order to avoid a model drift. This points out the importance of the experimental design that has to be consistent between the simulation used to compute the initial state and the hindcast initialised from this initial state. The hindcast including this constant additional freshwater flux provides trends in sea ice extent and concentration that are in satisfying agreement with satellite observations. This thus constitutes encouraging results for sea ice predictions in the Southern Ocean. In our simulation, the positive trend in ice extent over the last 30 years is largely determined by the state of the system in the late 1970's. No increase in meltwater flux from Antarctica is required.

1 Introduction

The sea ice extent in the Southern Ocean has been increasing at a rate of $17.1 \pm 2.3 \times 10^3 \, \mathrm{km^2 \, yr^{-1}}$ between November 1978 and December 2010 (Parkinson and Cavalieri, 2012). However, the processes that drive this evolution and the causes of sea

ice expansion are still debated. The hypothesis that the stratospheric ozone depletion (Solomon, 1999) could have been responsible for the increase in sea ice extent is not compatible with the results of recent analyses (e.g., Sigmond and Fyfe, 2010; Bitz and Polvani, 2012; Smith et al., 2012; Sigmond and Fyfe, 2013). Besides, other studies have underlined the fact that the positive trend in sea ice extent could be attributed to the internal variability of the system (e.g., Mahlstein et al., 2013; Zunz et al., 2013b; Polvani and Smith, 2013; Swart and Fyfe, 2013). Nevertheless, this explanation cannot be confirmed by present-day general circulation models (GCMs) involved in the 5th Coupled Model Intercomparison Project (CMIP5, Taylor et al., 2011). Indeed, because of the biases present in those models, they often simulate a seasonal cycle or an internal variability (or both) of the Southern Ocean sea ice that disagrees with what is observed (e.g., Turner et al., 2013; Zunz et al., 2013b).

Hypotheses related to changes in the atmospheric circulation or in the ocean stratification (e.g., Bitz et al., 2006; Zhang, 2007; Lefebvre and Goosse, 2008; Stammerjohn et al., 2008; Goosse et al., 2009; Kirkman and Bitz, 2010; Landrum et al., 2012; Holland and Kwok, 2012; Goosse and Zunz, 2014; de Lavergne et al., 2014) have also been proposed. In particular, a potential link between the melting of the Antarctic ice sheet, especially the ice shelves, and the formation of sea ice has been recently underlined (e.g., Hellmer, 2004; Swingedouw et al., 2008; Bintanja et al., 2013). The meltwater input from the ice sheet leads to a fresher and colder surface layer in the ocean surrounding Antarctica. As a consequence, the ocean gets more stratified and there is less interaction between the surface and the warmer and saltier interior ocean, leading to an enhanced cooling of the surface. This negative feedback could counteract the greenhouse warming and could thus contribute to the expansion of the sea ice. Estimates of the Antarctic ice sheet mass imbalance are available thanks to satellite observations and climate modelling. These estimates report an increase in the melting of the Antarctic ice sheet over the past decade, mainly coming from West Antarctica (e.g., Rignot et al., 2008; Velicogna, 2009; Pritchard et al., 2012; Shepherd et al., 2012). According to Bintanja et al. (2013), incorporating realistic changes in the Antarctic ice sheet mass

Decadal forecast skill of Southern Ocean sea ice

V. Zunz and H. Goosse

Title Page

Abstract	Introduction
Conclusions	References
Tables	Figures

|◄ | ►|

◄ | ►

Back | Close

Full Screen / Esc

Printer-friendly Version

Interactive Discussion

in a coupled climate model could lead to a better simulation of the evolution of the sea ice in the Southern Ocean. For past periods, this may be achieved using estimates of changes in mass balance but, for the future, this requires a comprehensive representation of the polar ice sheets in models. Besides, Swart and Fyfe (2013) have shown that the freshwater derived from the ice sheet is unlikely to affect significantly the recent trend in sea ice extent simulated by CMIP5 models, when imposing a flux whose magnitude is constrained by the observations.

In addition to the studies devoted to a better understanding of the causes of the recent variations, models are also employed to perform projection for the changes at the end of the 21st century and predictions for the next months to decades. Such predictions are generally performed using GCMs. Unfortunately, as mentioned above, current GCMs have biases that reduce the accuracy of the simulated sea ice in the Southern Ocean. In addition, taking into account observations to initialise these models, generally through simple data assimilation (DA) methods, did not improve the quality of the predictions in the Southern Ocean (Zunz et al., 2013b). However, two recent studies performed in a perfect model framework, i.e. using pseudo-observations provided by a reference simulation of the model instead of actual observations, underlined some predictability of the Southern Ocean sea ice (e.g., Holland et al., 2013; Zunz et al., 2013a). According to these studies, at interannual timescales, the predictability is limited to a few years ahead. Besides, significant predictability is found for the trends spanning several decades. Both studies have pointed out that the heat anomalies stored in the interior ocean could play a key role in the predictability of the sea ice. In particular, Zunz et al. (2013a) have underlined a link between the skill of the prediction of the sea ice cover and the quality of the initialisation of the ocean below it.

On the basis of those results, the present study aims at identifying a procedure that could improve the quality of the predictions of the sea ice in the Southern Ocean at multi-decadal timescales. Unlike Holland et al. (2013) and Zunz et al. (2013a), the results discussed here have been obtained in a realistic framework. It means that actual observations are used to initialise the model simulations as well as to assess the skill of

the model. The results of Holland et al. (2013) and Zunz et al. (2013b, a) encouraged us to focus on the prediction of the multi-decadal trends in sea ice concentration or extent rather than on its evolution at interannual timescales. Our study deals with two aspects that could influence the quality of the predicted trend in sea ice in the Southern Ocean: the initial state of the simulation and the magnitude of the freshwater input associated to the Antarctic ice sheet mass imbalance. The initialisation procedure is based on the nudging proposal particle filter (NPPF, Dubinkina and Goosse, 2013), a data assimilation method that requires large ensemble of simulations. Such a large amount of simulations cannot be afforded with GCMs because of their requirements in CPU time. We have thus chosen to work with an Earth-system model of intermediate complexity, LOVECLIM1.3. It has a coarser resolution and a lower level of complexity than a GCM, resulting in a lower computational cost. However, it behaves similarly to the GCMs in the Southern Ocean (Goosse and Zunz, 2014). It thus seems relevant to use this model to study the evolution of the Southern Ocean sea ice.

The climate model LOVECLIM1.3 is briefly described in Sect. 2.1, along with a summary of the simulations performed in this study. The data assimilation method used to compute the initial conditions of the hindcast simulations is presented in Sect. 2.2. Section 2.3 explains how the additional freshwater flux is taken into account in the simulations. Details about the measurement of the model skill are given in Sect. 2.4. The discussion of the results is divided into three parts: the simulations with data assimilation that provide the initial states (Sect. 3.1), the link between the freshwater flux applied during data assimilation and the model biases (Sect. 3.2) and the hindcast simulations (Sect. 3.3). Finally, Sect. 4 summarises the main results and proposes conclusions.

2 Methodology

2.1 Model and simulations

The three-dimensional Earth-system model of intermediate complexity LOVECLIM1.3 (Goosse et al., 2010) used here includes representations of the atmosphere (ECBilt2, Opsteegh et al., 1998), the ocean and the sea ice (CLIO3, Goosse and Fichefet, 1999) and the vegetation (VECODE, Brovkin et al., 2002). The atmospheric component is a T21 (corresponding to an horizontal resolution of about $5.6° \times 5.6°$), three-level quasi geostrophic model. The oceanic component consists of an ocean general circulation model coupled to a sea-ice model with horizontal resolution of $3° \times 3°$ and 20 unevenly spaced vertical levels in the ocean. The vegetation component simulates the evolution of trees, grasses and desert, with the same horizontal resolution as ECBilt2. The simulations performed in this study span the period 1850–2009 and are driven by the same natural and anthropogenic forcings (greenhouse gases increase, variations in volcanic activity, solar irradiance, orbital parameters and land use) as the ones adopted in the historical simulations performed in the framework of CMIP5 (Taylor et al., 2011).

Three kinds of simulation are performed in this study and all of them consist of 96-member ensembles. First, a simulation driven by external forcing only provides a reference to measure the predictive skill of the model that can be accounted for by the external forcing alone (NODA in Table 1). This numerical experiment does not take into account any observation, neither in its initialisation nor during the integration. At the initialisation and every three months of simulation, the surface air temperature of each members of NODA is slightly perturbed, to have an experimental design as close as possible to the simulations with data assimilation (see below). Second, simulations that assimilate observations of surface air temperature anomalies (see Sect. 2.2 for details) are used to reconstruct the past evolution of the system, from January 1850 to December 2009, and to provide initial conditions for hindcast simulations. Third, the hindcast simulations are initialised from a state the 1 January 1980 extracted from a simulation

with data assimilation and are not constrained by the observations during the model integration.

Two simulations with data assimilation, from 1850 to 2009, are analysed here: one without additional freshwater flux (DA_NOFWF in Table 1) and one that is forced by an autoregressive freshwater flux described in Sect. 2.3 (DA_FWF in Table 1), representing crudely the meltwater input to the Southern Ocean. The simulation DA_NOFWF provides the initial state of the first hindcast (HINDCAST_1 in Table 1) while the three other hindcasts (HINDCAST_2, HINDCAST_3 and HINDCAST_4 in Table 1) are initialised from a state extracted from DA_FWF. These three hindcasts differ to each other in the additional freshwater flux they receive during the model integration. No additional freshwater flux is applied for HINDCAST_2. HINDCAST_3 is forced by a time series resulting from the ensemble mean of the additional freshwater flux diagnosed in DA_FWF. The average over the period 1980–2009 of the ensemble mean diagnosed from DA_FWF is applied in HINDCAST_4 as a constant additional flux.

2.2 Data assimilation: the nudging proposal particle filter

Data assimilation consists of a combination of the model equations and the available observations, in order to provide an estimate of the state of the system as accurate as possible (Talagrand, 1997). The data assimilation simulations performed here provide a reconstruction of the past evolution of the climate system over the period 1850–2009. Such a long period appears necessary because of the long memory of the Southern Ocean. It allows the ocean to be dynamically consistent with the surface variables, constrained by the observations, over a wide depth range. The state of the system on 1 January 1980 is then extracted and used to initialise the hindcast. After the initialisation, the hindcast is driven by external forcing only and no observations are taken into account anymore.

In this study, observed anomalies of surface air temperature are assimilated in LOVE-CLIM1.3 thanks to a nudging proposal particle filter (Dubinkina and Goosse, 2013). The assimilated observations are from the HadCRUT3 dataset (Brohan et al., 2006).

V. Zunz and H. Goosse

Full Screen / Esc

Printer-friendly Version

Interactive Discussion

This dataset has been derived from in situ land and ocean observations and provides monthly values of surface air temperature anomalies (with regard to 1961–1990) since January 1850. Model anomalies of surface air temperature are computed with regard to a reference computed over 1961–1990 as well, from a simulation driven by the external forcing only, without data assimilation and additional freshwater flux.

The NPPF is based on the particle filter with sequential resampling (e.g., van Leeuwen, 2009; Dubinkina et al., 2011) that consists of three steps. First, an ensemble of simulations, the *particles*, is integrated forward in time with the model. These particles are initialised from a set of different initial conditions. Therefore, each particle represents a different solution of the model. Second, after three months of simulation, a weight is attributed to each particle of the ensemble based on its agreement with the observations. To compute this weight, only anomalies of surface air temperature southward of 30° S are taken into account. Third, the particles are resampled: the ones with small weight are eliminated while the ones with large weight are retained and duplicated, in proportion to their weight. This way, a constant number of particles is maintained throughout the procedure. A small perturbation is applied on the duplicated particles to generate different solutions of the model and the three steps are repeated until the end of the period of interest.

In the NPPF, a nudging is applied on each particle during the model integration. It consists of adding to the model equations a term that pulls the solution towards the observations (e.g., Kalnay, 2007). The nudging alone, i.e. not in combination with another DA method, has been used in many recent studies on decadal predictions (e.g., Keenlyside et al., 2008; Pohlmann et al., 2009; Dunstone and Smith, 2010; Smith et al., 2010; Kröger et al., 2012; Swingedouw et al., 2012; Matei et al., 2012; Servonnat et al., 2014). In LOVECLIM1.3, the nudging has been implemented as an additional heat flux between the atmosphere and the ocean $Q = \gamma(T_{mod} - T_{obs})$. T_{mod} and T_{obs} are the monthly mean surface air temperature simulated by the model and from the observations respectively. γ determines the relaxation time and equals $120\,\mathrm{W\,m^{-2}\,K^{-1}}$, a value similar to the ones used in other studies (e.g., Keenlyside et al., 2008; Pohlmann et al.,

Full Screen / Esc

Printer-friendly Version

Interactive Discussion

2009; Smith et al., 2010; Matei et al., 2012; Swingedouw et al., 2012; Servonnat et al., 2014). The nudging is applied on every ocean grid cell, except the ones covered by sea ice and the amplitude of the nudging applied on a particle is taken into account in the computation of its weight (Dubinkina and Goosse, 2013).

2.3 Autoregressive additional freshwater flux

As the freshwater related to the melting of the Antarctic ice sheet may contribute to the variability of the sea ice extent (e.g., Hellmer, 2004; Swingedouw et al., 2008; Bintanja et al., 2013), it appears relevant to check its impact on the data assimilation simulations as well as on the hindcasts. However, deriving the distribution of the freshwater flux from estimate of the observed Antarctic ice sheet mass imbalance is not possible for the whole period covered by our simulations, because of the lack of data. Furthermore, the configuration of the model used in our study does not allow simulating this freshwater flux in an interactive way. We have thus chosen to apply a random freshwater flux, described in term of an autoregressive process as in Mathiot et al. (2013), on each particle during the data assimilation simulation DA_FWF (see Table 1 for details). This allows determining the most adequate value of the additional freshwater flux for the model using the NPPF. Because of this additional freshwater flux, the parameters selected to define the error covariance matrix, required to compute the weight of each particle (see Dubinkina et al., 2011), are slightly modified in comparison to the values applied for these parameters in the data assimilation without additional freshwater flux (DA_NOFWF).

The freshwater flux is computed every three months, i.e. with the same frequency as the particle filtering, as follow:

$$\text{FWF}(t) = \text{FWF}(t-1) + 0.25\epsilon_{\text{FWF}}(t-1) + \epsilon_{\text{FWF}}(t) \tag{1}$$

where ϵ_{FWF} is a random noise following a Gaussian distribution $N(0, \sigma_{\text{FWF}})$, with σ_{FWF} equal to 10 mSv. The parameters of the autoregressive process have been chosen in

order to obtain a freshwater flux compatible with the estimates of the current Antarctic ice sheet mass loss.

The melting of the Antarctic ice sheet being particularly strong over West Antarctica (e.g., Rignot et al., 2008; Velicogna, 2009; Pritchard et al., 2012; Shepherd et al., 2012), we have chosen to distribute uniformly the freshwater flux in the ocean between 0° and 170° W, southern of 70° S (area in blue on Fig. 1). Here, the distribution of the freshwater flux is thus not limited to the cells adjacent to the Antarctic shelf, unlike Bintanja et al. (2013); Swart and Fyfe (2013). This is based on the assumption that a part of the freshwater might be redistributed offshore by icebergs (e.g., Silva et al., 2006) or coastal currents not well represented in a coarse-resolution model. Alternatively, we can also consider that the ice sheet mass imbalance is not the only contributor to the additional freshwater flux required by the model. For instance, variations in precipitation are also expected to impact the freshwater balance in the Southern Ocean and might not be simulated adequately by the model.

This freshwater flux increases the range of solutions reached by the particles and could randomly bring some of them closer to the observations. When a particle is picked up because of its large weight, it is duplicated and the copied particles inherit of the value of the freshwater flux that possibly brought the particle close to the observations. This value keeps influencing the copied particles because the freshwater flux is autoregressive. It could thus improve the efficiency of the particle filter. Furthermore, by selecting the solutions that best fit the observations, the particle filter allows estimating the freshwater flux that is more likely to provide a state compatible with the observations.

2.4 Skill assessment

In order to measure the skill of the model combined with the assimilation of observations, the results of the data assimilation simulations and of the hindcasts are compared to observations of the annual mean sea ice concentration (the fraction of grid cell covered by sea ice) and sea ice extent (the sum of the areas of all grid cells having

Title Page

Abstract | Introduction

Conclusions | References

Tables | Figures

|◄ | ►|

◄ | ►

Back | Close

Full Screen / Esc

Printer-friendly Version

Interactive Discussion

a sea ice concentration above 15 %), between 1980 and 2009. This corresponds to the period for which reliable observations of the whole ice covered area are available. The sea ice concentration data used here are derived from the Nimbus-7 SMMR and DMSP SSM/I-SSMIS satellite observations through the bootstrap algorithm (Comiso, 1999, updated daily). The sea ice extent is provided by the Sea Ice Index from the National Snow and Ice Data Center (Fetterer et al., 2002, updated daily).

Particular attention is paid on the trend in sea ice concentration and extent. Significance levels for the trends are computed on the basis of a two-tailed t test. The autocorrelation of the residuals is taken into account in both the standard deviation of the trend and in the number of degrees of freedom used to to determine the significance threshold (e.g., Santer et al., 2000; Stroeve et al., 2012). This statistical test provides an estimate of the relative significance of the trend, but we have to keep in mind that the assumptions inherent to this kind of test are rarely totally satisfied in the real world (e.g., Santer et al., 2000).

The ensemble means computed for the results of the data assimilation simulations consists of weighted averages. The ensemble mean $X(y,m)$ of the variable x, for the month m in the year y is thus defined as

$$X(y,m) = \frac{1}{K} \sum_{k=1}^{K} x_k(y,m) . w_k(y,m), \tag{2}$$

where k is the member index, K is the number of members within the ensemble and $w_k(y,m)$ is the weight attributed to the member k during the data assimilation procedure. The ensemble means of each month of the year are then averaged over a year to obtain the annual mean.

The standard deviation of the annual mean of the ensemble cannot be computed explicitly because of the possible time discontinuity in the results of individual members, arising from the resampling occurring every three months. An estimate of this standard deviation is however assessed by multiplying the weighted standard deviation of each month of a year by a coefficient and averaging it over the year. These coefficients are

Title Page

Abstract	Introduction
Conclusions	References
Tables	Figures

| ◄◄ | ►► |
| ◄ | ► |

| Back | Close |

Full Screen / Esc

Printer-friendly Version

Interactive Discussion

introduced to take into account the fact that the standard deviation of the annual mean is not the mean of the standard deviation from every month. They are obtained here by computing the mean ratio between the ensemble standard deviation of the annual mean and the ensemble standard deviation of each month in the simulation NODA.

5   The ensemble means and standard deviations calculated for NODA and for the hind-cast simulations correspond to classical values that does not include any weight as this procedure is only required when data assimilation is applied.

3   Results

In this section, the results of the various simulations (see Table 1 for details) are dis-

10 cussed. First, the reconstruction of the evolution of the sea ice between 1850 and 2009, provided by the simulations NODA, DA_NOFWF and DA_FWF, is presented in Sect. 3.1 and compared to observations. Second, the link between the model biases and the freshwater flux diagnosed from the data assimilation is presented in Sect. 3.2. Third, the hindcasts initialised with a state extracted from a data assimilation simu-

15 lation are analysed to measure the skill of the prediction system tested in this study (Sect. 3.3).

3.1   Data assimilation simulations

The observations of yearly mean sea ice extent display a positive trend between 1980 and 2009 (Fig. 2) equal to $17.4 \times 10^3 \, \text{km}^2 \, \text{yr}^{-1}$, significant at the 99 % level. This trend

20 in sea ice extent is the result of an increase in sea ice concentration in most part of the Southern Ocean, particularly in the Ross Sea (Fig. 3a).

    When no data assimilation is included in the model simulation (NODA), the ensemble mean displays a decreasing trend in sea ice extent in response to the external forcing (Fig. 2a and b), similar to the one found in other climate models (e.g., Zunz

25 et al., 2013b). Consequently, for the ensemble mean, 30-years trends are negative

during the whole period of the simulation without data assimilation (Fig. 2b). Over the period 1980–2009, the ensemble mean of the trend in sea ice extent equals $-15.5 \times 10^3 \, \text{km}^2 \, \text{yr}^{-1}$, with an ensemble standard deviation of $14.5 \times 10^3 \, \text{km}^2 \, \text{yr}^{-1}$, and the melting of sea ice occurs everywhere in the Southern Ocean (Fig. 3b), except in the Ross Sea and in the Western Pacific sector. This negative trend obtained for the ensemble mean is the result of a wide range of behaviours simulated by the different members belonging to the ensemble (light green shade in Fig. 2a and b) and, considered individually, the members can thus provide positive or negative values for the trend. This indicates thus that, for some members, the natural variability could compensate for the negative trend in sea ice extent simulated in response to the external forcing. Positive trends similar to the one observed over the last 30 years are however rare in NODA. For instance, only 14 of the 96 members have a positive trend over the period 1980–2009 and none of them have a trend larger than the observed one.

In NODA, the ensemble mean displays an increase in the heat contained in both the upper ocean, defined here as the first 100 m below the surface, and the interior ocean, considered to lie between -100 and -500 m (green solid line in Fig. 4a). The correlation between these two variables equals 0.86 over the period 1980–2009 (Table 2). This warming of the ocean results directly from the increase in the external forcing and is consistent with the decrease in sea ice extent (Fig. 2a). Besides, the ocean salt content in the first 100 m decreases (Fig. 4b). This is likely due to the enhanced hydrological cycle in a global warming context and the inherent increase in precipitations at high southern latitudes that freshens the ocean surface (e.g., Liu and Curry, 2010; Fyfe et al., 2012). In the simulation NODA, the negative correlation of -0.92 between the ocean heat and salt content in the first 100 m below the surface over the period 1980–2009 (see Table 2) is linked to the response of these two variables to the external forcing.

If observations of the anomalies of the surface air temperature are assimilated during the simulation, without additional freshwater flux (DA_NOFWF), the model is able to capture the observed interannual and multi-decadal variability of this variable, as ex-

pected (Fig. 5b). Consequently, the trend in the ensemble mean sea ice extent is more variable than in NODA. Over the period 1850–2009, the values of the 30 year trend in sea ice extent, computed from the ensemble mean, stand between $-29.1 \times 10^3 \, \text{km}^2 \, \text{yr}^{-1}$ and $13.6 \times 10^3 \, \text{km}^2 \, \text{yr}^{-1}$ (Fig. 2d). Between 1980 and 2009, the trend in sea ice extent equals $-3.0 \times 10^3 \, \text{km}^2 \, \text{yr}^{-1}$. On average over the ensemble, the trend is thus less negative than in the case where no observation are taken into account during the simulation but it still has a sign opposite to the observed one. Nevertheless, the trends in sea ice concentration display a pattern roughly similar to the observed one (Fig. 3a and c), with an increase in the Weddell Sea, in the eastern Indian sector, in the Western Pacific sector and in the Ross Sea, the sea ice concentration decreasing elsewhere. The decrease in sea ice concentration occurring in the Bellingshausen and Amundsen Seas is, however, overestimated by the model, leading to the decrease of the overall extent.

In the simulation DA_NOFWF, the ocean heat content in both the upper and interior ocean is lower than the ones obtained in the simulation NODA until about 1980 (Fig. 4a and b). This arises from the lower surface air temperature in DA_NOFWF compared to NODA (Fig. 5a and b) that cools down the whole system. The correlation between the upper and interior ocean heat contents equals 0.25 over the period 1980–2009 (Table 2) and is thus lower than in NODA. This could be due to the interannual variability captured thanks to the data assimilation that mitigates the global warming signal (see below). The ocean salt content is larger in DA_NOFWF than in NODA until 1980, likely because of the weakening of the hydrological cycle associated to the lower simulated temperature. From 1980 ahead, the ocean heat content, in both the upper and middle layer, increases and the salt content decreases in response to the external forcing, as in NODA. Nevertheless, as the ocean heat content is still slightly lower in the simulation DA_NOFWF than in the simulation NODA, the quantity of energy available to melt the sea ice at the surface is also lower. This can explain why the absolute value of the trend in sea extent between 1980 and 2009 is smaller in DA_NOFWF than in NODA.

Including a freshwater flux following an autoregressive process in the data assimilation simulation (DA_FWF), as described in Sect. 2.3, increases the number of degrees of freedom of the modelled system and stimulates the variability of the ensemble mean sea ice extent, at both interannual and multi-decadal timescales (Fig. 2e and f). This is particularly clear before 1950, i.e. during the time period over which less observations are available to constrain the model (Dubinkina and Goosse, 2013). Over the period 1850–2009, the ensemble mean of the 30 year trend in sea ice extent varies between $-68.3 \times 10^3 \, \text{km}^2 \, \text{yr}^{-1}$ and $70.9 \times 10^3 \, \text{km}^2 \, \text{yr}^{-1}$. Between 1980 and 2009, the average simulated trend equals $14.7 \times 10^3 \, \text{km}^2 \, \text{yr}^{-1}$ (not significant at the 99 % level), which is very close to the observed value of $17.4 \times 10^3 \, \text{km}^2 \, \text{yr}^{-1}$. In addition, the distribution of the trend in sea ice concentration, between 1980 and 2009, fits well the observations (Fig. 3a and d). In particular, the decrease in sea ice concentration occurring in the Bellingsausen and Amundsen seas is weaker than in DA_NOFWF and it is thus in better agreement with satellite data. We should detail here that this good match with observed trends is obtained from the constraints provided by (scarce) surface temperature observations, as no sea ice data is used in the assimilation process. Besides, the anomalies of the sea ice extent, with regard to the simulation NODA, have a mean of $-0.42 \times 10^6 \, \text{km}^2$ over the period 1980–2009. This shift in the mean state of the sea ice is discussed in Sect. 3.2.

In DA_FWF, the correlation between the heat content in the upper ocean (Fig. 4a) and the one in the interior ocean (Fig. 4b) has a negative value of -0.82 over the period 1980–2009 (see Table 2). It means that when the ocean surface is colder, the middle layer is warmer and vice-versa. This suggests that the evolution of the distribution of the heat content in the water column critically depends on the exchanges between the surface and the interior of the ocean, the impact of the external forcing being apparently weaker than in DA_NOFWF. The amplitude of the mixing depends on the difference in density between the surface and the deeper layers, which is in turn determined by the difference in temperature and salinity. In the simulation DA_FWF, the correlation between the ocean salt and heat contents in the first 100 m reaches a value of 0.76,

while it is negative in NODA and in DA_NOFWF (see Table 2). This confirms that, during periods of increase in salt content in the upper layer, the vertical mixing in the ocean is enhanced, allowing positive heat anomalies to be transported from the interior to the upper ocean. The heat content in the first 100 m increases while the one between

5 −100 m and −500 m decreases. On the contrary, when the salt content in the upper layer decreases, the ocean becomes more stratified, preventing the heat exchange between the surface and the interior ocean. The heat is trapped in the interior ocean that gets warmer, and the upper ocean cools down.

Because of the additional freshwater flux that tends to stabilise the water column dur-

10 ing some periods and to destabilise it in others (Fig. 6), the general behaviour of the ocean in the simulation DA_FWF differs from the simulation NODA and DA_NOFWF. While the latter simulations appear mainly driven by the external forcing, the interaction between the different layers in the ocean seems to be dominant in DA_FWF. In the simulation DA_FWF, the ocean heat and salt contents of the surface layer are particularly

15 large in 1980 while the heat content between 100 and 500 m is low. This implies that the heat storage at depth is much lower in DA_FWF than in NODA. Note that the heat content of the top 500 m in DA_FWF is also lower than in NODA. After 1980, the salt content decreases until 2009 (Fig. 4c). This is associated with a decrease in the upper ocean heat content and a strong increase in the ocean temperature between 100 and

20 500 m, suggesting a reduction of the vertical ocean heat flux. This is likely responsible for the increase in sea ice extent between 1980 and 2009 (Fig. 2e). In DA_FWF, the additional freshwater flux is the main cause of the variability of the stratification. Additionally, internal processes can be responsible for such changes in vertical exchanges, as discussed in details in Goosse and Zunz (2014), also leading to a negative correla-

25 tion between the heat content in surface and intermediate layers. This explains why the correlation between those two variables is lower for the ensemble mean of DA_NOFWF than in NODA. It is also much lower in individual simulation of NODA (0.02 on average, Table 2) than in the ensemble mean (0.86, Table 2), the ensemble mean amplifying the contribution of the response to the forcing associated with high positive value.

3.2 Model biases and freshwater flux

Over the years 1980–2009, the model, without data assimilation, simulates too cold a surface air temperature on average over the box southward of 30° S compared to the reference period 1961–1990, i.e. a mean anomaly over 1980–2009 of 0.06 °C in NODA against 0.13 °C in the observations. Besides, the model is much too warm before 1960. This bias is clearly reduced in the two data assimilation simulations DA_NOFWF and DA_FWF, that furthermore provide a better synchronisation between the model solutions and the observations (Fig. 5). Nevertheless, this bias reduction is likely achieved differently whether an additional freshwater flux is included or not during the data assimilation. If no additional freshwater flux is taken into account, the shift in the model state induced by the data assimilation procedure is partly due to the nudging and partly to the selection of the particles whose simulated temperature is closer to the observations. The sea ice simulated by a particle is then linked to the surface air temperature through the model dynamics. Adding a freshwater flux during the data assimilation process modifies the structure of the ocean that in turn impacts the sea ice formation and the temperature at the ocean surface. The covariance between the sea ice and the surface air temperature is thus modified. However, the particles are still selected on the basis of the agreement between the surface air temperature they simulate and the observed one. As a consequence, the state of the mean surface air temperature simulated in DA_NOFWF is very similar to the one in DA_FWF but the state of the sea ice differs between these two data assimilation simulation, the simulation DA_FWF displaying a lower sea ice extent over the period 1980–2009.

On average over the period 1850–2009, the weighted ensemble mean of the freshwater flux diagnosed from the simulation DA_FWF is negative (−0.02 Sv, Fig. 6). The freshwater flux also displays a large amplitude of variation (standard deviation over the period 1850–2009 = 0.03 Sv), that decreases after 1980 likely thanks to the stronger constraints provided by the observations of surface air temperature. Indeed, until 1950, the assimilated observations are scarce (Dubinkina and Goosse, 2013) and the fresh-

water flux obtained before 1950 should thus be interpreted cautiously. Over the period 1980–2009, the freshwater flux equals −0.03 Sv on average. This mean negative flux is relatively small compared to the standard deviation over the whole period but likely participates to the model bias reduction over the period 1980–2009. Indeed, a negative freshwater flux makes the ocean surface saltier and destabilises the water column. This enhances the vertical mixing and warmer water from the interior ocean reaches the surface that consequently warms up. Therefore, particles receiving a negative freshwater flux are more likely to get closer to the observations compared to the mean of NODA that is too cold over this period. They have thus a higher probability to be selected by the particle filter, reducing the model bias.

The negative value obtained for the ensemble mean of the freshwater flux between 1980 and 2009 may appear in contradiction with the estimates of the Antarctic ice sheet mass imbalance. Indeed, these clearly indicate a melting of the ice sheet that results in a freshwater input in the Southern Ocean. Nevertheless, the freshwater flux applied in our simulation allows first to compensate for model biases thanks to this negative mean value. Starting from a negative value in 1980, the ensemble mean of the freshwater flux slightly increases until 2009 at a rate of 4.53×10^{-5} Sv yr^{-1}, equivalent to a change in melting rate of 42 Gt yr^{-1} between 1980 and 2009 (Fig. 6). This value is much smaller than the increase in freshwater flux derived from the recent estimates of the ice sheet mass imbalance but the values are only available on shorter timescales. For instance, in their reconciled estimates, Shepherd et al. (2012) reported a freshwater input from the West-Antarctic ice sheet melting of 38 ± 32 Gt yr^{-1} ($\simeq 10^{-3}$ Sv) over 1992–2000 and of 102 ± 18 Gt yr^{-1} ($\simeq 3 \times 10^{-3}$ Sv) over 2005–2010. To sum up, our results show that the mean value of the additional freshwater flux does impact the simulation results by compensating for model biases but the increase in this flux may not be a determinant feature.

3.3 Hindcast simulations

In this section, we focus on simulations that are initialised on 1 January 1980 with a state that has been extracted from the data assimilation simulations discussed in Sect. 3.1. After the initialisation, the hindcast simulation is driven by external forcing but no observation is taken into account anymore. The analyses discussed here aims at answering two questions. (1) Can the information contained in the initial state persist long enough to impact the simulated trend in sea ice extent? (2) How does an additional freshwater flux impact the sea ice in hindcast simulations? Including an additional freshwater flux appears indeed to be relevant to improve the efficiency of data assimilation (see Sect. 3.1). The results of HINDCAST_1, initialised from DA_NOFWF, and of HINDCAST_2, initialised from DA_FWF, bring answers to the first question, these hindcasts including no additional freshwater flux. The second question is specifically addressed in the analyses of HINDCAST_3 and HINDCAST_4. Both are initialised from a state provided by the simulation DA_FWF and include an additional freshwater flux. Given that it is still not clear whether it is the mean value of the additional freshwater flux or its variations that matters, two configurations for the additional freshwater flux have been tested. In HINDCAST_3, the additional freshwater flux corresponds to the one that has been diagnosed from DA_FWF, shown on Fig. 6, and evolves in time. On the contrary, in HINDCAST_4, the freshwater flux is constant in time and equals -0.03 Sv, the average freshwater flux diagnosed in DA_FWF between 1980 and 2009.

In HINDCAST_1, the sea ice extent is high at the beginning of the simulation and decreases between 1980 and 2009 (Fig. 7a). The ensemble mean of the trends equals $-14.2 \times 10^3 \, \text{km}^2 \, \text{yr}^{-1}$, with an ensemble standard deviation of $13.2 \times 10^3 \, \text{km}^2 \, \text{yr}^{-1}$. This provides a 95 % range that does not encompass the observed trend of $17.4 \times 10^3 \, \text{km}^2 \, \text{yr}^{-1}$. In this hindcast, the trend in sea ice concentration is negative over a large area in the Bellingshausen and Amundsen Seas and slightly positive elsewhere (Fig. 8a). This pattern thus roughly fits the observed one but the decrease obtained in the western part of the Southern Ocean covers too large an area. The regional distri-

bution of the trend in sea ice concentration in HINDCAST_1 (Fig. 8a) is very similar to the one in DA_NOFWF, i.e. the simulation that provided the initial state for HIND-CAST_1. This suggests that the information provided at the initialisation can impact the solution of the hindcast over multi-decadal timescales, in agreement with the re-
5 sults discussed in Zunz et al. (2013a). The too large decrease in sea ice concentration occurring in the Bellingshausen and Amundsen Seas already noticed in DA_NOFWF is however amplified in HINDCAST_1, leading to an overall decrease similar to the mean of NODA.

The ocean heat and salt contents in HINDCAST_1 follow roughly the evolution of
10 these variables for the ensemble mean in NODA (Fig. 4). The correlation between the upper and interior ocean heat content equals 0.82 and the correlation between the upper ocean heat and salt content equals -0.93 (see Table 2). This points out the role played by the external forcing in this hindcast, as dicussed in Sect. 3.1.

By contrast, the results of HINDCAST_2 display a low sea ice extent at the beginning
15 of the simulation (Fig. 7b). During the first 5 years following the initialisation, the sea ice extent rapidly increases until the solution reaches the model climatology and then re-mains more or less stable. Overall, the trend in sea ice extent between 1980 and 2009 computed from this hindcast has an ensemble mean equal to $19.1 \times 10^3 \, \mathrm{km^2 \, yr^{-1}}$ and a standard deviation of $15.7 \times 10^3 \, \mathrm{km^2 \, yr^{-1}}$. The ensemble is thus shifted towards posi-
20 tive values of the trend in sea ice extent compared to HINDCAST_1, with an ensemble mean that is very close to the observed one. This positive value is, however, mainly due to the model drift caused by a change in the conditions of the experiment compared to DA_FWF that provided the initial state. As HINDCAST_2 is not driven by any additional freshwater flux, the sea ice extent rapidly tends to its mean climatological state in this
25 configuration: this is the one obtained in NODA which is characterised by a higher ice extent than in DA_FWF. The model drift is also clearly seen in the ocean heat and salt contents (Fig. 4a and b).

The regional distribution of the trend in sea ice concentration is in good agreement with the observations (Fig. 8b). Nevertheless, this apparent satisfying results provided

by HINDCAST_2 has to be moderated given the drift that produces unrealistic trends at the beginning of the simulation.

In HINDCAST_3, the additional freshwater flux applied during the simulations slows down the increase in sea ice extent at the beginning of the simulation (Fig. 7c), re-sulting in a weaker trend compared to HINDCAST_2 (Fig. 7b). The ensemble mean (standard deviation) of the trends equals $5.1 \times 10^3 \, \text{km}^2 \, \text{yr}^{-1}$ ($15.5 \times 10^3 \, \text{km}^2 \, \text{yr}^{-1}$), the observed value of $17.4 \times 10^3 \, \text{km}^2 \, \text{yr}^{-1}$ is thus well within the ensemble range. The trend is relatively stable over the whole 30 year period and not concentrated on the first years of simulation, as in HINDCAST_2. Furthermore, the exprimental conditions are much closer to DA_FWF. There is thus no reason to suspect that the increase in sea ice ex-tent in HINDCAST_3 is due to a spurious drift. Such a weak or even non existent drift is ensured by the experimental design, consistent with the behaviour of the ocean heat and salt contents that remain relatively far from the results of NODA (Fig. 4).

The pattern of the trend in sea ice concentration reasonably fits the observations (Fig. 8c). Including an additional freshwater flux during the hindcast simulation ensures thus a compensation of the model biases, as in the simulation DA_FWF, and avoids the generation of unrealistic trend just after the initialisation. This improves the results of the hindcast but the method applied in HINDCAST_3 requires using information spanning the period being predicted to determine the time evolution of the additional freshwater flux.

The additional freshwater flux applied during the simulation HINDCAST_4, equal to $-0.03 \, \text{Sv}$, corresponds to the mean of the diagnosed freshwater flux over the period 1980–2009 in DA_FWF and thus does not require a detailed knowledge of its variation in time. Note that this value is very close to the one of the period preceeding the hindcast. The trend in sea ice extent in HINDCAST_4 has an ensemble mean equal to $1.9 \times 10^3 \, \text{km}^2 \, \text{yr}^{-1}$ and a standard deviation of $16.6 \times 10^3 \, \text{km}^2 \, \text{yr}^{-1}$ (Fig. 7d). The ensemble mean of the trend is thus slightly smaller than the one of HINDCAST_3 but the ensemble still contains the observed trend. Furthermore, the sea ice extent does not display a rapid change during the first years of simulation. This suggests

that the model drift is also prevented by the addition of a constant freshwater flux during the hindcast simulation. The ocean heat and salt contents stay relatively far from the model climatology (Fig. 4), confirming the absence of a significant model drift in HINDCAST_4.

The regional distribution of the trend in sea ice concentration is in a satisfying agreement with the observed one (Fig. 8d). This last hindcast thus provides trends in sea ice extent and concentration that fit the observations. Forcing the hindcast with a mean value for the additional freshwater flux also allows compensating for model biases and avoids model drift. Therefore, while adding a freshwater flux is needed to maintain the sea ice of the hindcast around a mean state compatible with the initial state, a detailed knowledge of the time evolution of the freshwater flux does not seem to be crucial.

4   Summary and conclusions

In our simulations, assimilating anomalies of the surface air temperature through the nudging proposal particle filter induces an increase in the trend in simulated sea ice extent over recent decades in the Southern Ocean, compared to the case where no observation is taken into account. This leads to a better agreement with satellite data than in the simulation without data assimilation, the latter displaying a reduction of the extent in response to the forcing. Further improvement is achieved if an additional autoregressive freshwater flux is included during the data assimilation. This freshwater flux allows compensating for model deficiencies that affect the representation of the freshwater cycle (in particular the variability of the meltwater input), the ocean dynamics, the internal variability, etc. In combination with the data assimilation, the additional freshwater input leads to simulated trends in sea ice extent and concentration between 1980 and 2009 that reproduce well the observations. The freshwater flux thus appears to play an important role on the simulated evolution of the sea ice, as already pointed out in previous studies (e.g., Hellmer, 2004; Swingedouw et al., 2008; Bintanja et al., 2013).

Hindcasts initialised from those simulations with data assimilation have allowed illustrating factors that can potentially increase the model skill to predict the trend in Southern Ocean sea ice over the next decades. This is summarised into three points below.

1. Initialising a hindcast simulation with a state extracted from a simulation that has assimilated observations through a nudging proposal particle filter has a significant impact on the simulated trends in sea ice extent and concentration over the period 1980–2009. This indicates that the information contained in the initial state influences the results of the simulation over multi-decadal timescales, confirming the results of Zunz et al. (2013a). As a consequence, an initial condition that adequately represents the observed state is required in order to perform skillful predictions for the trend in sea ice extent over the next decades. Nevertheless, the conclusions drawn from our hindcast simulations have to be considered cautiously since they are based on the analyses of the only 30 year period for which we have relevant observations. Similar analyses could be performed for periods starting before 1980, using the reconstruction of the sea ice provided by the simulation with data assimilation as target for the hindcast instead of actual observations. However, this approach would be nearly equivalent to a perfect model study, as proposed in Zunz et al. (2013a).

2. It has been shown that the experimental design used to perform a prediction has to be consistent with the one applied in the simulation providing the initial state for the forecast simulation. In particular, a shift in the mean state of the sea ice has been pointed out in the simulation with data assimilation and additional freshwater flux, that could lead to a model drift in the hindcast initialised from this simulation. Such a drift could be prevented if a freshwater flux of amplitude similar to the one applied during the simulation with data assimilation is included in the hindcast simulation.

3. In hindcast simulations, the variations in the freshwater flux diagnosed through the data assimilation are not needed to simulate a positive trend in ice extent over the last decades. A time average of the freshwater flux leads to results similar to the ones obtained when the variations are taken into account. The time evolution of the additional freshwater flux has thus little impact on the hindcast simulations, in agreement with the results of Swart and Fyfe (2013). The strong link between the freshwater input derived from the melting of the Antarctic ice sheet and the increase in sea ice extent between 1980 and 2009, suggested by Bintanja et al. (2013), is thus not confirmed in the present study.

Those results indicate that the increase in ice extent, the surface cooling and the freshening simulated between 1980 and 2009, in both simulations with data assimilation and hindcasts using additional freshwater flux, could not be attributed to the anthropogenical forcing or to a particular large melting of the ice sheet during this period. The evolution of the variables at the surface of the ocean after 1980 seems rather influenced by the state of the ocean in the 1970's, characterised by a warm and salty surface layer, a cold intermediate layer and a strong convection. This state is consistent with the results of de Lavergne et al. (2014) and evolves towards a fresher and cooler upper ocean that allows a greater production of sea ice. In our experiments, this state in the late 1970's is reached thanks to variations in the freshwater input to the Southern Ocean. This flux is very likely playing a role but we could not determine if it is amplified or not by our experimental design that allows variations of this flux only and not of other forcings or model parameters. Whether the addition of a freshwater flux could compensate for biases in the simulated sea ice in other climate models still needs to be investigated, a reduction of the model biases being also possible through other approaches. Overall, the results that have been discussed here are rather encouraging and open perspectives to perform predictions of the sea ice in the Southern Ocean over the next decades.

References

Bintanja, R., van Oldenborgh, G. J., Drijfhout, S. S., Wouters, B., and Katsman, C. A.: Important role for ocean warming and increased ice-shelf melt in Antarctic sea-ice expansion, Nat. Geosci., 6, 376–379, 2013. 3565, 3571, 3572, 3584, 3586

Bitz, C. M. and Polvani, L. M.: Antarctic climate response to stratospheric ozone depletion in a fine resolution ocean climate model, Geophys. Res. Lett., 39, L20705, doi:10.1029/2012GL053393, 2012. 3565

Bitz, C. M., Gent, P. R., Woodgate, R. A., Holland, M. M., and Lindsay, R.: The influence of sea ice on ocean heat uptake in response to increasing CO_2, J. Climate, 19, 2437–2450, 2006. 3565

Brohan, P., Kennedy, J. J., Harris, I., Tett, S. F. B., and Jones, P. D.: Uncertainty estimates in regional and global observed temperature changes: A new data set from 1850, J. Geophys. Res., 111, D12106, doi:10.1029/2005JD006548, 2006. 3569, 3599

Brovkin, V., Bendtsen, J., Claussen, M., Ganopolski, A., Kubatzki, C., Petoukhov, V., and Andreev, A.: Carbon cycle, vegetation, and climate dynamics in the Holocene: experiments with the CLIMBER-2 model, Global Biogeochem. Cy., 16, 1139, doi:10.1029/2001GB001662, 2002. 3568

Comiso, J.: Bootstrap Sea Ice Concentrations from Nimbus-7 SMMR and DMSP SSM/I-SSMIS. Version 2, January 1980 to December 2009, NASA DAAC at the National Snow and Ice Data Center, Boulder, Colorado, USA, 1999, updated daily. 3573, 3597

de Lavergne, C., Palter, J. B., Galbraith, E. D., Bernardello, R., and Marinov, I.: Cessation of deep convection in the open Southern Ocean under anthropogenic climate change, Nature Clim., 4, 278–282, 2014. 3565, 3586

Title Page

Abstract | Introduction

Conclusions | References

Tables | Figures

◀ | ▶

◀ | ▶

Back | Close

Full Screen / Esc

Printer-friendly Version

Interactive Discussion

Dubinkina, S. and Goosse, H.: An assessment of particle filtering methods and nudging for climate state reconstructions, Clim. Past, 9, 1141–1152, doi:10.5194/cp-9-1141-2013, 2013. 3567, 3569, 3571, 3577, 3579

Dubinkina, S., Goosse, H., Sallaz-Damaz, Y., Crespin, E., and Crucifix, M.: Testing a particle filter to reconstruct climate changes over the past centuries, Int. J. Bifurcat. Chaos, 21, 3611–3618, doi:10.1142/S0218127411030763, 2011. 3570, 3571

Dunstone, N. J. and Smith, D. M.: Impact of atmosphere and sub-surface ocean data on decadal climate prediction, Geophys. Res. Lett., 37, L02709, doi:10.1029/2009GL041609, 2010. 3570

Fetterer, F., Knowles, K., Meier, W., and Savoie, M.: Sea Ice Index, January 1980 to December 2009, National Snow and Ice Data Center, Boulder, Colorado USA, doi:10.7265/N5QJ7F7W, 2002, updated daily. 3573, 3596, 3601

Fyfe, J. C., Gillett, N. P., and Marshall, G. J.: Human influence on extratropical Southern Hemisphere summer precipitation, Geophys. Res. Lett., 39, L23711, doi:10.1029/2012GL054199, 2012. 3575

Goosse, H. and Fichefet, T.: Importance of ice–ocean interactions for the global ocean circulation: IA model study, J. Geophys. Res.-Oceans, 104, 23337–23355, 1999. 3568

Goosse, H. and Zunz, V.: Decadal trends in the Antarctic sea ice extent ultimately controlled by ice–ocean feedback, The Cryosphere, 8, 453–470, doi:10.5194/tc-8-453-2014, 2014. 3565, 3567, 3578

Goosse, H., Lefebvre, W., de Montety, A., Crespin, E., and Orsi, A.: Consistent past half-century trends in the atmosphere, the sea ice and the ocean at high southern latitudes, Clim. Dynam., 33, 999–1016–1016, 2009. 3565

Goosse, H., Brovkin, V., Fichefet, T., Haarsma, R., Huybrechts, P., Jongma, J., Mouchet, A., Selten, F., Barriat, P.-Y., Campin, J.-M., Deleersnijder, E., Driesschaert, E., Goelzer, H., Janssens, I., Loutre, M.-F., Morales Maqueda, M. A., Opsteegh, T., Mathieu, P.-P., Munhoven, G., Pettersson, E. J., Renssen, H., Roche, D. M., Schaeffer, M., Tartinville, B., Timmermann, A., and Weber, S. L.: Description of the Earth system model of intermediate complexity LOVECLIM version 1.2, Geosci. Model Dev., 3, 603–633, doi:10.5194/gmd-3-603-2010, 2010. 3568

Hellmer, H. H.: Impact of Antarctic ice shelf basal melting on sea ice and deep ocean properties, Geophys. Res. Lett., 31, L10307, doi:10.1029/2004GL019506, 2004. 3565, 3571, 3584

Title Page

Abstract | Introduction

Conclusions | References

Tables | Figures

|◄ | ►|

◄ | ►

Back | Close

Full Screen / Esc

Printer-friendly Version

Interactive Discussion

Holland, M. M., Blanchard-Wrigglesworth, E., Kay, J., and Vavrus, S.: Initial-value predictability of Antarctic sea ice in the Community Climate System Model 3, Geophys. Res. Lett., 40, 2121–2124, doi:10.1002/grl.50410, 2013. 3566, 3567

Holland, P. R. and Kwok, R.: Wind-driven trends in Antarctic sea-ice drift, Nat. Geosci., 5, 872–875, 2012. 3565

Kalnay, E.: Atmospheric Modeling, Data Assimilation and Predictability, 4th edn., Cambridge University Press, Cambridge, 2007. 3570

Keenlyside, N., Latif, M., Jungclaus, J. H., Kornbueh, L., and Roeckner, E.: Advancing decadal-scale climate prediction in the North Atlantic sector, Nature, 453, 84–88, 2008. 3570

Kirkman, C. H. and Bitz, C. M.: The effect of the sea ice freshwater flux on Southern Ocean temperatures in CCSM3: deep-ocean warming and delayed surface warming, J. Climate, 24, 2224–2237, 2010. 3565

Kröger, J., Müller, W., and von Storch, J.-S.: Impact of different ocean reanalyses on decadal climate prediction, Clim. Dynam., 39, 795–810, 2012. 3570

Landrum, L., Holland, M. M., Schneider, D. P., and Hunke, E.: Antarctic sea ice climatology, variability, and late twentieth-century change in CCSM4, J. Climate, 25, 4817–4838, 2012. 3565

Lefebvre, W. and Goosse, H.: An analysis of the atmospheric processes driving the large-scale winter sea ice variability in the Southern Ocean, J. Geophys. Res., 113, C02004, doi:10.1029/2006JC004032, 2008. 3565

Liu, J. and Curry, J. A.: Accelerated warming of the Southern Ocean and its impacts on the hydrological cycle and sea ice, P. Natl. Acad. Sci. USA, 107, 14987–14992, 2010. 3575

Mahlstein, I., Gent, P. R., and Solomon, S.: Historical Antarctic mean sea ice area, sea ice trends, and winds in CMIP5 simulations, J. Geophys. Res.-Atmos., 118, 1–6, doi:10.1002/jgrd.50443 2013. 3565

Matei, D., Pohlmann, H., Jungclaus, J., Müller, W., Haak, H., and Marotzke, J.: Two tales of initializing decadal climate prediction experiments with the ECHAM5/MPI-OM model, J. Climate, 25, 8502–8523, 2012. 3570, 3571

Mathiot, P., Goosse, H., Crosta, X., Stenni, B., Braida, M., Renssen, H., Van Meerbeeck, C. J., Masson-Delmotte, V., Mairesse, A., and Dubinkina, S.: Using data assimilation to investigate the causes of Southern Hemisphere high latitude cooling from 10 to 8 ka BP, Clim. Past, 9, 887–901, doi:10.5194/cp-9-887-2013, 2013. 3571

Title Page

Abstract | Introduction

Conclusions | References

Tables | Figures

◀ | ▶

Back | Close

Full Screen / Esc

Printer-friendly Version

Interactive Discussion

Opsteegh, J. D., Haarsma, R., Selten, F., and Kattenberg, A.: ECBILT: a dynamic alternative to mixed boundary conditions in ocean models, Tellus A, 50, 348–367, 1998. 3568

Parkinson, C. L. and Cavalieri, D. J.: Antarctic sea ice variability and trends, 1979–2010, The Cryosphere, 6, 871–880, doi:10.5194/tc-6-871-2012, 2012. 3564

Pohlmann, H., Jungclaus, J. H., Köhl, A., Stammer, D., and Marotzke, J.: Initializing decadal climate predictions with the GECCO oceanic synthesis: effects on the North Atlantic, J. Climate, 22, 3926–3938, 2009. 3570

Polvani, L. M. and Smith, K. L.: Can natural variability explain observed Antarctic sea ice trends? New modeling evidence from CMIP5, Geophys. Res. Lett., 40, 3195–3199, 2013. 3565

Pritchard, H. D., Ligtenberg, S. R. M., Fricker, H. A., Vaughan, D. G., van den Broeke, M. R., and Padman, L.: Antarctic ice-sheet loss driven by basal melting of ice shelves, Nature, 484, 502–505, 2012. 3565, 3572

Rignot, E., Bamber, J. L., van den Broeke, M. R., Davis, C., Li, Y., van de Berg, W. J., and van Meijgaard, E.: Recent Antarctic ice mass loss from radar interferometry and regional climate modelling, Nat. Geosci., 1, 106–110, 2008. 3565, 3572

Santer, B. D., Wigley, T. M. L., Boyle, J. S., Gaffen, D. J., Hnilo, J. J., Nychka, D., Parker, D. E., and Taylor, K. E.: Statistical significance of trends and trend differences in layer-average atmospheric temperature time series, J. Geophys. Res., 105, 7337–7356, doi:10.1029/1999JD901105, 2000. 3573

Servonnat, J., J. Mignot, E. Guilyardi, D. Swingedouw, R. Séférian, and S. Labetoulle (2014), Reconstructing the subsurface ocean decadal variability using surface nudging in a perfect model framework, Clim. Dynam., 1–24, doi:10.1007/s00382-014-2184-7, 2014. 3570, 3571

Shepherd, A., Ivins, E. R., A, G., Barletta, V. R., Bentley, M. J., Bettadpur, S., Briggs, K. H., Bromwich, D. H., Forsberg, R., Galin, N., Horwath, M., Jacobs, S., Joughin, I., King, M. A., Lenaerts, J. T. M., Li, J., Ligtenberg, S. R. M., Luckman, A., Luthcke, S. B., McMillan, M., Meister, R., Milne, G., Mouginot, J., Muir, A., Nicolas, J. P., Paden, J., Payne, A. J., Pritchard, H., Rignot, E., Rott, H., Sørensen, L. S., Scambos, T. A., Scheuchl, B., Schrama, E. J. O., Smith, B., Sundal, A. V., van Angelen, J. H., van de Berg, W. J., van den Broeke, M. R., Vaughan, D. G., Velicogna, I., Wahr, J., Whitehouse, P. L., Wingham, D. J., Yi, D., Young, D., and Zwally, H. J.: A reconciled estimate of ice-sheet mass balance, Science, 338, 1183–1189, doi:10.1126/science.1228102, 2012. 3565, 3572, 3580

Decadal forecast skill of Southern Ocean sea ice

V. Zunz and H. Goosse

Title Page

Abstract	Introduction
Conclusions	References
Tables	Figures

◁◁ ▷▷

◁ ▷

Back Close

Full Screen / Esc

Printer-friendly Version

Interactive Discussion

Sigmond, M. and Fyfe, J. C.: Has the ozone hole contributed to increased Antarctic sea ice extent?, Geophys. Res. Lett., 37, L18502, doi:10.1029/2010GL044301, 2010. 3565

Sigmond, M. and Fyfe, J. C.: The Antarctic sea ice response to the ozone hole in climate models, J. Climate, 27, 1336–1342, 2013. 3565

5 Silva, T. A. M., Bigg, G. R., and Nicholls, K. W.: Contribution of giant icebergs to the Southern Ocean freshwater flux, J. Geophys. Res.-Oceans, 111, C03004, doi:10.1029/2004JC002843, 2006. 3572

Smith, D. M., Eade, R., Dunstone, N. J., Fereday, D., Murphy, J. M., Pohlmann, H., and Scaife, A. A.: Skilful multi-year predictions of Atlantic hurricane frequency, Nat. Geosci., 3,
10 846–849, 2010. 3570, 3571

Smith, K. L., Polvani, L. M., and Marsh, D. R.: Mitigation of 21st century Antarctic sea ice loss by stratospheric ozone recovery, Geophys. Res. Lett., 39, L20701, doi:10.1029/2012GL053325, 2012. 3565

Solomon, S.: Stratospheric ozone depletion: a review of concepts and history, Rev. Geophys.,
15 37, 275–316, 1999. 3565

Stammerjohn, S. E., Martinson, D. G., Smith, R. C., Yuan, X., and Rind, D.: Trends in Antarctic annual sea ice retreat and advance and their relation to El Niño Southern Oscillation and Southern Annular Mode variability, J. Geophys. Res., 113, C03S90, doi:10.1029/2007JC004269, 2008. 3565

20 Stroeve, J. C., Kattsov, V., Barrett, A., Serreze, M., Pavlova, T., Holland, M., and Meier, W. N.: Trends in Arctic sea ice extent from CMIP5, CMIP3 and observations, Geophys. Res. Lett., 39, L16502, doi:10.1029/2012GL052676, 2012. 3573

Swart, N. C. and Fyfe, J. C.: The influence of recent Antarctic ice sheet retreat on simulated sea ice area trends, Geophys. Res. Lett., 40, 4328–4332, 2013. 3565, 3566, 3572, 3586

25 Swingedouw, D., Fichefet, T., Huybrechts, P., Goosse, H., Driesschaert, E., and Loutre, M.-F.: Antarctic ice-sheet melting provides negative feedbacks on future climate warming, Geophys. Res. Lett., 35, L17705, doi:10.1029/2008GL034410, 2008. 3565, 3571, 3584

Swingedouw, D., Mignot, J., Labetoulle, S., Guilyardi, E., and Madec, G.: Initialisation and predictability of the AMOC over the last 50 years in a climate model, Clim. Dynam., 2381–2399,
30 doi:10.1007/s00382-012-1516-8. 2012. 3570, 3571

Talagrand, O.: Assimilation of observations, an introduction, J. Meteorol. Soc. Jpn., 75, 191–209, 1997. 3569

Title Page

Abstract | Introduction

Conclusions | References

Tables | Figures

◄ | ►

Back | Close

Full Screen / Esc

Printer-friendly Version

Interactive Discussion

Taylor, K. E., Stouffer, R. J., and Meehl, G. A.: An overview of CMIP5 and the experiment design, B. Am. Meteorol. Soc., 93, 485–498, 2011. 3565, 3568

Turner, J., Bracegirdle, T. J., Phillips, T., Marshall, G. J., and Hosking, J. S.: An initial assessment of Antarctic sea ice extent in the CMIP5 models, J. Climate, 26, 1473–1484, doi:10.1175/JCLI-D-12-00068.1, 2013. 3565

van Leeuwen, P. J.: Particle filtering in geophysical systems, Mon. Weather Rev., 137, 4089–4114, doi:10.1175/2009MWR2835.1, 2009. 3570

Velicogna, I.: Increasing rates of ice mass loss from the Greenland and Antarctic ice sheets revealed by GRACE, Geophys. Res. Lett., 36, L19503, doi:10.1029/2009GL040222, 2009. 3565, 3572

Zhang, J.: Increasing Antarctic sea ice under warming atmospheric and oceanic conditions, J. Climate, 20, 2515–2529, 2007. 3565

Zunz, V., Goosse, H., and Dubinkina, S.: Impact of the initialisation on the predictability of the Southern Ocean sea ice at interannual to multi-decadal timescales, Clim. Dynam., submitted, 2013a. 3566, 3567, 3582, 3585

Zunz, V., Goosse, H., and Massonnet, F.: How does internal variability influence the ability of CMIP5 models to reproduce the recent trend in Southern Ocean sea ice extent?, The Cryosphere, 7, 451–468, doi:10.5194/tc-7-451-2013, 2013b. 3565, 3566, 3567, 3574

Title Page

Abstract | Introduction

Conclusions | References

Tables | Figures

◀ | ▶

◀ | ▶

Back | Close

Full Screen / Esc

Printer-friendly Version

Interactive Discussion

Table 1. Summary of the simulations analysed in this study. All the simulations are 96-member ensembles.

Simulation	Time period	Initialisation	Data assimilation	Additional freshwater flux during the simulation
NODA	Jan 1850–Dec 2009	on 1 Jan 1850	NO	NO
DA_NOFWF	Jan 1850–Dec 2009	on 1 Jan 1850	YES	NO
DA_FWF	Jan 1850–Dec 2009	on 1 Jan 1850	YES	Autoregressive FWF
HINDCAST_1	Jan 1980–Dec 2009	on 1 Jan 1980 from DA_NOFWF	NO	NO
HINDCAST_2	Jan 1980–Dec 2009	on 1 Jan 1980 from DA_FWF	NO	NO
HINDCAST_3	Jan 1980–Dec 2009	on 1 Jan 1980 from DA_FWF	NO	Ensemble mean of the FWF computed in DA_FWF between 1980 and 2009 (see Fig. 6).
HINDCAST_4	Jan 1980–Dec 2009	on 1 Jan 1980 from DA_FWF	NO	Ensemble mean of the FWF computed in DA_FWF, averaged over the period 1980–2009 (= −0.03 Sv).

Table 2. Correlation between the ocean heat content in the first 100 m below the surface and the ocean heat content between −500 m and −100 m (2nd column) and correlation between the ocean heat content and the ocean salt content in the first 100 m below the surface (3rd column), for the different simulations summarised in Table 1. The correlation is computed over the period 1980 and 2009, from the ensemble mean of the variables. For the simulation NODA, the correlation computed for each member of the simulation and averaged over the ensemble is given in brackets.

Simulation	Correlation between the upper and interior ocean heat content	Correlation between the upper ocean heat and salt contents
NODA	0.86 (0.02)	−0.92 (−0.03)
DA_NOFWF	0.25	−0.22
DA_FWF	−0.82	0.76
HINDCAST_1	0.82	−0.93
HINDCAST_2	−0.92	0.86
HINDCAST_3	−0.43	0.42
HINDCAST_4	−0.25	0.31

Figure 1. Spatial distribution of the additional freshwater flux included in model simulations.
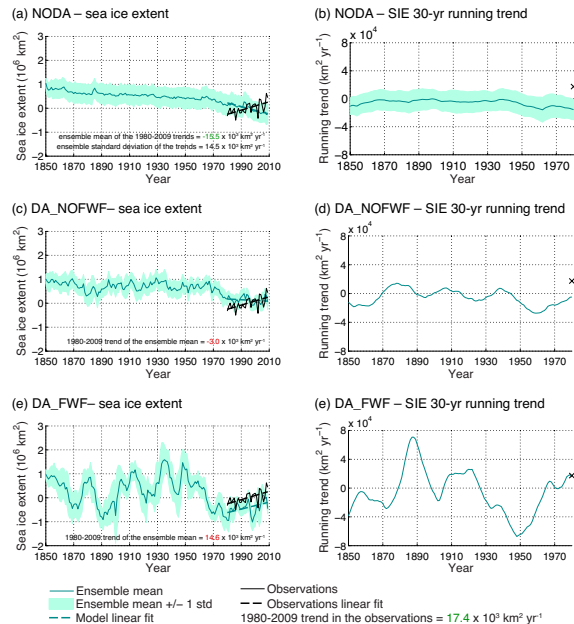
Figure 2. (a, c, e) Yearly mean sea ice extent anomalies with regard to 1980–2009 and **(b, d, f)** 30 year running trend in sea ice extent. Results are from **(a, b)** the simulation without data assimilation (NODA), **(c, d)** the model simulation that assimilates anomalies of surface air temperature (DA_NOFWF) and **(e, f)** the model simulation that assimilates anomalies of surface air temperature and that is forced by an additional autoregressive freshwater flux (DA_FWF). The model ensemble mean is shown as the dark green line surrounded by one standard deviation shown as the light green shade. Observations (Fetterer et al., 2002, updated daily) are shown as the black line (cross) in **(a, c, e)** (in **b, d, f**). The green (black) dashed line shows the linear fit of the model simulation (observations) in **(a, c, e)**. The values of the trend indicated in the (**a, c** and **e**) correspond to the ensemble mean of the trends along with the ensemble standard deviation for NODA. Trends that are (non-)significant at the 99 % level are shown in green (red).
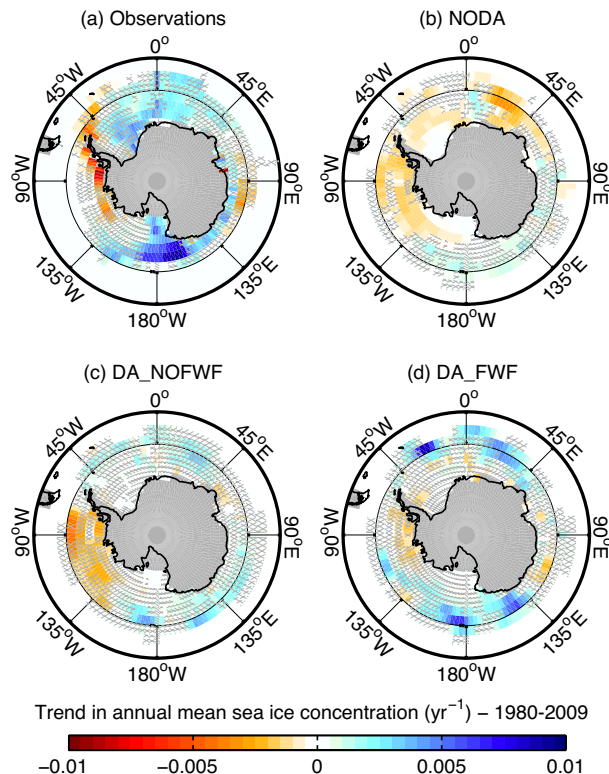
Figure 3. Trend in yearly mean sea ice concentration between 1980 and 2009, shown for **(a)** the observations (Comiso, 1999, updated daily), **(b)** the model simulation without data assimilation (NODA), **(c)** the model simulation that assimilates anomalies of surface air temperature (DA_NOFWF) and **(d)** the model simulation that assimilates anomalies of surface air temperature and that is forced by an additional autoregressive freshwater flux (DA_FWF). Hatched areas highlight the grid cells where the trend is not significant at the 99 % level. The shaded grey areas correspond to the land mask of the ocean model.
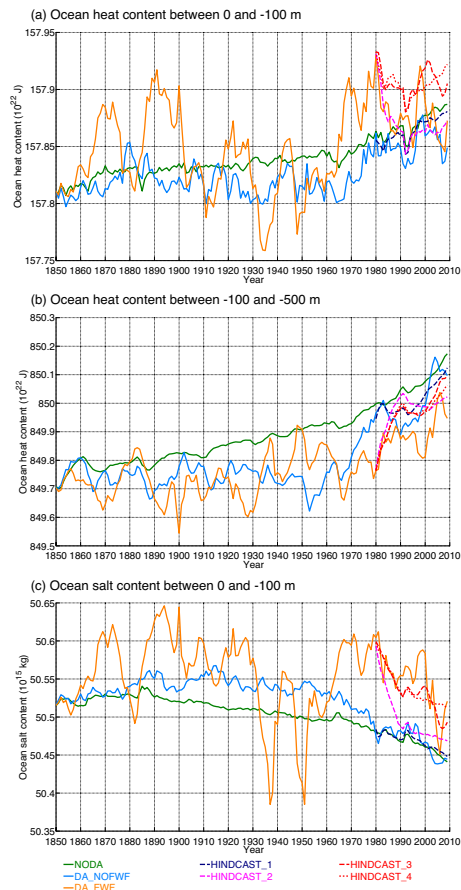
Figure 4. Ensemble mean of yearly mean **(a)** ocean heat content in the first 100 m below the surface, **(b)** ocean heat content between −100 and −500 m and **(c)** ocean salt content in the first 100 m below the surface, for the simulations summarised in Table 1. The ocean heat and salt contents are computed southward of 60° S.

Title Page

Abstract | Introduction

Conclusions | References

Tables | Figures

|◀ | ▶|

◀ | ▶

Back | Close

Full Screen / Esc

Printer-friendly Version

Interactive Discussion
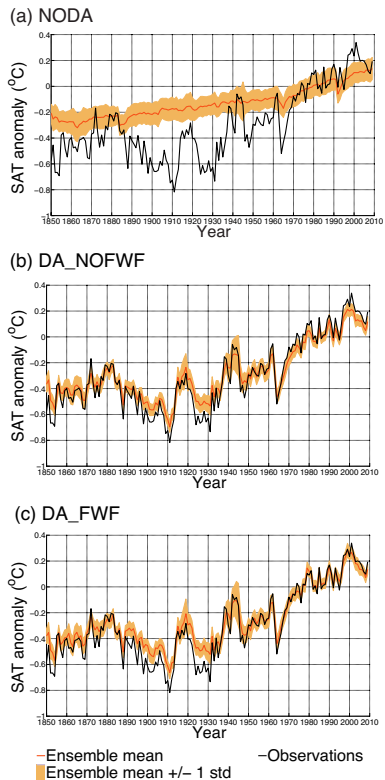
Figure 5. Yearly mean surface air temperature anomalies with regard to 1961–1990, averaged over the area southward of 30° S, from **(a)** the model simulation without data assimilation (NODA), **(b)** the model simulation that assimilates anomalies of surface air temperature (DA_NOFWF) and **(c)** the model simulation that assimilates anomalies of surface air temperature and that is forced by an additional autoregressive freshwater flux (DA_FWF). The model ensemble mean is shown as the orange line, surrounded by one standard deviation shown as the light orange shade. Observations (Brohan et al., 2006) are shown as the black line.

Decadal forecast skill of Southern Ocean sea ice

V. Zunz and H. Goosse

Title Page

Abstract	Introduction
Conclusions	References
Tables	Figures

|◄ | ►|

◄ | ►

Back | Close

Full Screen / Esc

Printer-friendly Version

Interactive Discussion
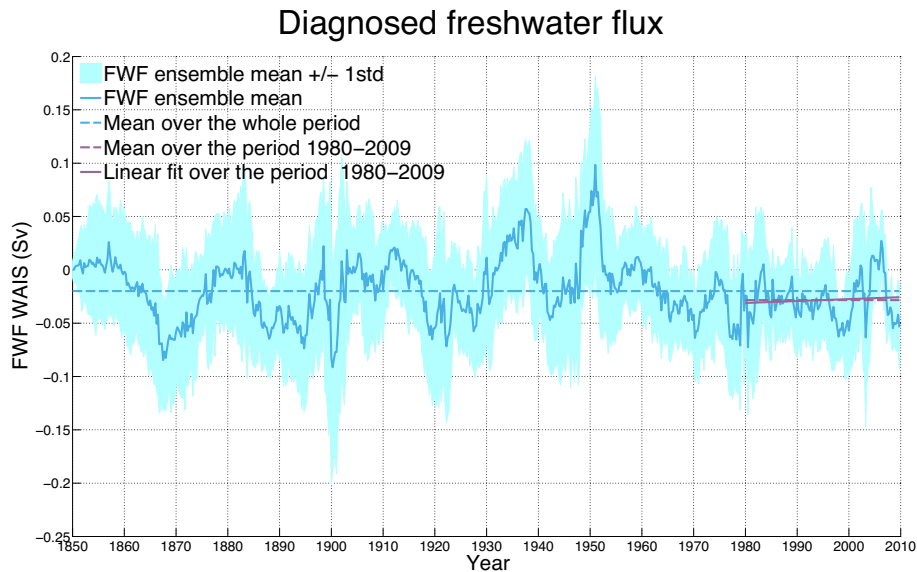
Figure 6. Freshwater flux from the model simulation with data assimilation and additional autoregressive freshwater flux (DA_FWF). The ensemble mean is shown as the blue solid line, surrounded by one standard deviation shown as the light blue shade. The dashed blue (purple) line shows the mean over the period 1850–2009 (1980–2009). The linear fit between 1980 and 2009 is shown as the solid purple line.
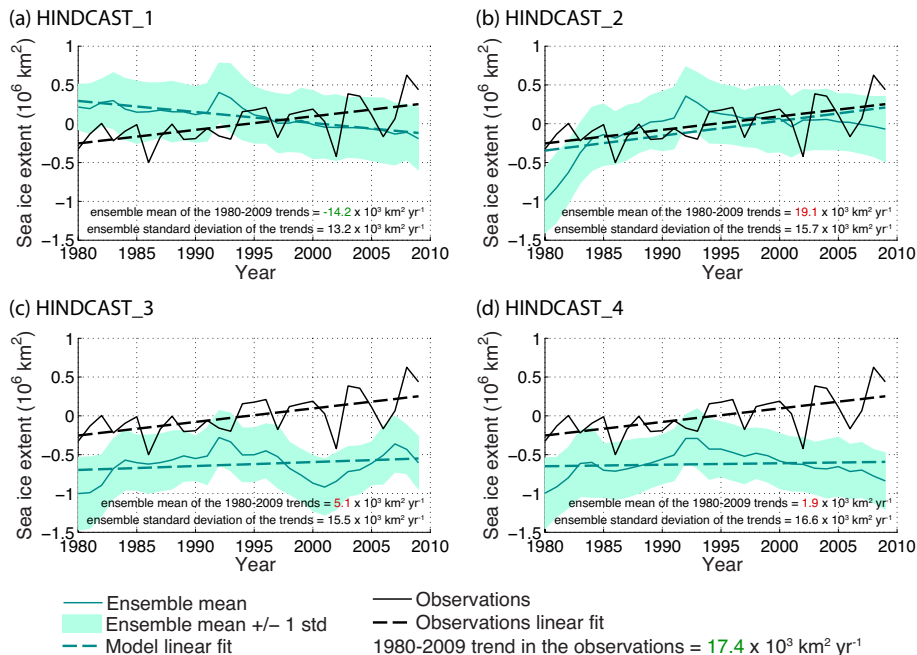
Figure 7. Yearly mean sea ice extent anomalies with regard to 1980–2009, for the four hindcast simulations initialised on 1 January 1980 through data assimilation (see Table 1 for details). The model ensemble mean is shown as the dark green line, surrounded by one standard deviation shown as the light green shade. Observations (Fetterer et al., 2002, updated daily) are shown as the black line. The green (black) dashed line shows the linear fit of the model simulation (observations). The values of the trend indicated in each panel correspond to the ensemble mean of the trends along with the ensemble standard deviation. Trends that are (non-)significant at the 99 % level are shown in green (red).

Title Page

Abstract | Introduction

Conclusions | References

Tables | Figures

|◄ | ►|

◄ | ►

Back | Close

Full Screen / Esc

Printer-friendly Version

Interactive Discussion
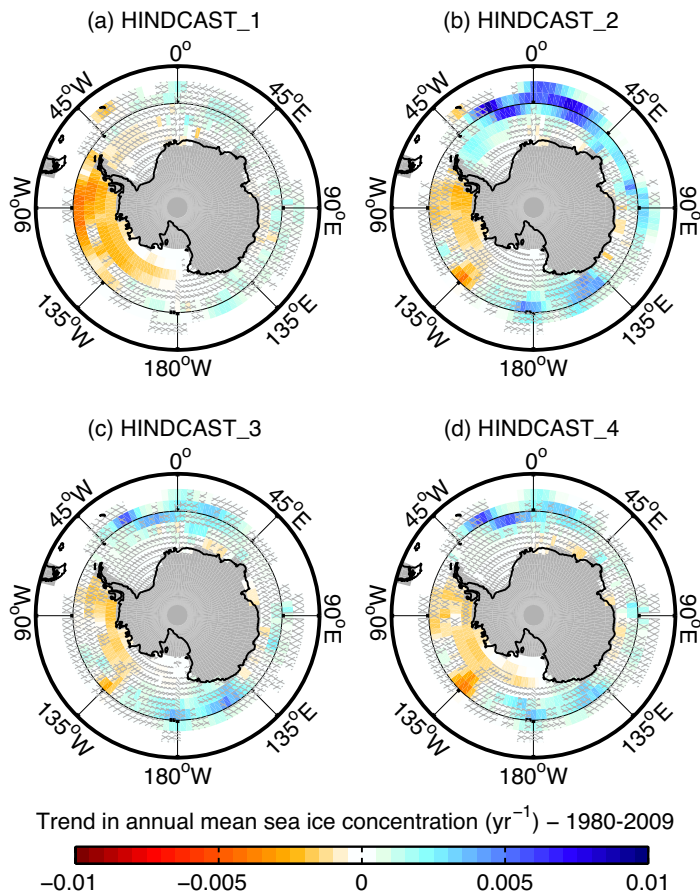
Figure 8. Trend in yearly mean sea ice concentration between 1980 and 2009, for the four hindcast simulations initialised on 1 January 1980 through data assimilation (see Table 1 for details). Hatched areas highlight the grid cells where the trend is not significant at the 99 % level. The shaded grey areas correspond to the land mask of the ocean model.

Title Page

Abstract | Introduction

Conclusions | References

Tables | Figures

|◄ | ►|

◄ | ►

Back | Close

Full Screen / Esc

Printer-friendly Version

Interactive Discussion